



## Search for $t\bar{t}$ Resonances in the Lepton+Jets Final State in $p\bar{p}$ Collisions at $\sqrt{s} = 1.96$ TeV

The DØ Collaboration  
URL <http://www-d0.fnal.gov>  
(Dated: March 8, 2008)

A search for a narrow-width heavy resonance decaying into top quark pairs ( $X \rightarrow t\bar{t}$ ) in  $p\bar{p}$  collisions at  $\sqrt{s} = 1.96$  TeV has been performed using data collected with the DØ detector at the Fermilab Tevatron Collider. This analysis considers  $t\bar{t}$  candidate events in the lepton+jets channel using a neural network tagger to identify  $b$ -jets and the  $t\bar{t}$  invariant mass distribution to search for evidence of resonant production. The analyzed dataset corresponds to an integrated luminosity of approximately  $2.1 \text{ fb}^{-1}$ . We find no evidence for a narrow resonance  $X$  decaying to  $t\bar{t}$ . Therefore, we set upper limits on  $\sigma_X \cdot B(X \rightarrow t\bar{t})$  for different hypothesized resonance masses using a Bayesian approach. Within a topcolor-assisted technicolor model, the existence of a leptophobic  $Z'$  boson with mass  $M_{Z'} < 760$  GeV and width  $\Gamma_{Z'} = 0.012M_{Z'}$  can be excluded at 95% C.L.

*Preliminary Result for Winter 2008 Conferences*

## I. INTRODUCTION

The top quark has by far the largest mass of all the known fermions. Heavy, yet unknown resonances may play a role in the production of top pairs and add a resonant part to the Standard Model mechanism. Such resonant production is possible for massive  $Z$ -like bosons in extended gauge theories [1], Kaluza Klein states of the gluon or  $Z$  boson [2, 3], axigluons [4], topcolor [5], and other theories beyond the Standard Model. Independent of the exact model, resonant production should be visible in the  $t\bar{t}$  invariant mass distribution, a wide low mass resonance will be very hard to notice in the  $t\bar{t}$  spectrum.

In this note a search for a narrow-width heavy resonance  $X$  decaying into  $t\bar{t}$  is presented. We consider the lepton+jets ( $\ell$ +jets, where  $\ell = e$  or  $\mu$ ) final state. The event signature is one isolated electron or muon with high transverse momentum ( $p_T$ ), large transverse energy imbalance ( $\cancel{E}_T$ ) due to the undetected neutrino, and at least three jets, two of which result from the hadronization of  $b$  quarks.

The analyzed D0 data set includes about  $0.9 \text{ fb}^{-1}$  from Tevatron Run IIa (August 2002 to December 2005) and about  $1.2 \text{ fb}^{-1}$  from Run IIb (January 2006 to July 2007). The total integrated luminosity for the  $e$ +jets ( $\mu$ +jets) is  $2115 \text{ fb}^{-1}$  ( $2073 \text{ fb}^{-1}$ ). The signal-to-background ratio is improved by identifying  $b$ -jets using a neural network based  $b$ -tagging algorithm. After  $b$ -tagging, the dominant physics background for a resonance signal is non-resonant SM  $t\bar{t}$  production. Smaller contributions arise from the direct production of  $W$  bosons in association with four or more jets ( $W$ +jets), as well as instrumental background originating from multijet processes with jets faking isolated leptons.

The search for a resonance in the  $t\bar{t}$  invariant mass distribution is performed using a Bayesian ansatz to compare standard model with resonant production.

Previous searches performed by CDF and D0 in Run I found no evidence for a  $t\bar{t}$  resonance [6, 7]. In these studies a top-color model was used as a reference for quoting mass limits. According to the model described in [5] a large top quark mass can be generated through the formation of a dynamical  $t\bar{t}$  condensate,  $X$ , due to a new strong gauge force coupling preferentially to the third generation of fermions. In one particular model, top-color-assisted technicolor [8], the  $X$  boson couples weakly and symmetrically to the first and second generations but strongly to the third generation of quarks, and has no couplings to leptons. Thus the SM  $q\bar{q}$  annihilation process is augmented by a resonance contribution from  $X$  decay. Limits obtained on  $\sigma_X \cdot B(X \rightarrow t\bar{t})$  are used to set a lower bound on the mass of such a top-color  $Z'$  boson. In Run I CDF found  $M_{Z'} > 480 \text{ GeV}$  with  $106 \text{ pb}^{-1}$  of data [6] and D0 obtained  $M_{Z'} > 560 \text{ GeV}$  using  $130 \text{ pb}^{-1}$  [7], both at 95% C.L. and for a resonance with  $\Gamma_X = 0.012M_X$ . The most recent results yield  $M_{Z'} > 690 \text{ GeV}$  for the D0 analysis [9] with  $900 \text{ pb}^{-1}$  and  $M_{Z'} > 725 \text{ GeV}$  for the CDF analysis with  $680 \text{ pb}^{-1}$  [10] and  $M_{Z'} > 720 \text{ GeV}$  with  $955 \text{ pb}^{-1}$  [11], all for a resonance with  $\Gamma_X = 0.012M_X$ .

## II. DØ DETECTOR

The D0 detector [12] has a central-tracking system consisting of a silicon microstrip tracker and a central fiber tracker, both located within a 2 T superconducting solenoidal magnet, with designs optimized for tracking and vertexing at pseudorapidities  $|\eta| < 3$  and  $|\eta| < 2.5$  respectively. Central and forward preshower detectors are positioned just outside of the superconducting coil. A liquid-argon and uranium calorimeter has a central section (CC) covering pseudorapidities  $|\eta|$  up to  $\approx 1.1$ , and two end calorimeters (EC) that extend coverage to  $|\eta| \approx 4.2$ , with all three housed in separate cryostats [13]. An outer muon system, at  $|\eta| < 2$ , consists of a layer of tracking detectors and scintillation trigger counters in front of 1.8 T toroids, followed by two similar layers after the toroids [14]. Luminosity is measured using plastic scintillator arrays placed in front of the EC cryostats. The trigger and data acquisition systems are designed to accommodate the high luminosities of Run II.

## III. EVENT SELECTION

To select top pair events in the  $e$ +jets and  $\mu$ +jets decay channels, triggers that required a jet and an electron or muon are used. Offline we require either an isolated electron with  $p_T > 20 \text{ GeV}$  and  $|\eta| < 1.1$ , or an isolated muon with  $p_T > 20 \text{ GeV}$  and  $|\eta| < 2.0$ . No additional isolated leptons with  $p_T > 15 \text{ GeV}$  are allowed in the event [15, 16]. We require  $\cancel{E}_T$  to exceed  $20 \text{ GeV}$  ( $25 \text{ GeV}$ ) for the  $e$ +jets ( $\mu$ +jets) channel and to not be collinear with the lepton direction in the transverse plane. Jets are defined using a cone algorithm [17] with radius  $R_{cone} = 0.5$ , where  $R_{cone} = \sqrt{\Delta\phi^2 + \Delta y^2}$ ,  $\phi$  is the azimuthal angle, and  $y$  is the rapidity. The selected events must contain three or more jets with  $p_T > 20 \text{ GeV}$  and  $|\eta| < 2.5$ . One of the jets is required to have  $p_T > 40 \text{ GeV}$  and, for the Run IIb data set, a charged particle fraction from the primary vertex above 0.75 [18]. In the muon+jets channel, events with a mismeasured muon momentum are rejected by requiring  $\Delta\phi(\mu, \cancel{E}_T) > 2.1 - 0.035 \cancel{E}_T$ , where  $\Delta\phi(\mu, \cancel{E}_T)$  denotes the azimuthal angle between the muon and  $\cancel{E}_T$  directions. Also events where a second muon gives an invariant mass of

the two muons within 70 to 100 GeV are rejected. In the electron+jets channel, events with a mismeasured electron momentum are rejected by requiring  $\Delta\phi(e, \cancel{E}_T) > 2.2 - 0.045 \cancel{E}_T$ .

In order to improve the signal-to-background ratio, at least one jet is required to be identified as a  $b$ -jet. The tagging algorithm uses the impact parameters of tracks matched to a given jet, information on vertex mass, the significance of displacement, and the number of participating tracks for any reconstructed secondary vertex within the cone of the given jet. The output variable,  $NN_B$ , is near one for  $b$ -jets and near zero for light jets [19]. In this analysis we consider jets as  $b$ -tagged if  $NN_B > 0.65$  which corresponds to a tagging efficiency for  $b$ -jets of about 55% at a rate for light partons (u, d, s, g) of less than 1%. We independently analyze singly  $b$ -tagged and doubly  $b$ -tagged events since the channels have different systematic uncertainties.

#### IV. SIGNAL AND BACKGROUND MODELING

Simulated events are used to determine selection efficiencies for the resonant  $t\bar{t}$  production signal and for background sources except those in which instrumental effects give fake leptons and  $\cancel{E}_T$  in multijet production events.

Samples of resonant  $t\bar{t}$  production are generated with PYTHIA 6.409 [20] for Run IIb and with PYTHIA 6.323 for Run IIa each for ten different choices of the resonance mass  $M_X$  between 350 GeV and 1.2 TeV. In all cases, the width of the resonance is set to  $\Gamma_X = 0.012M_X$ . This qualifies the  $X$  boson as a narrow resonance since its width is smaller than the expected mass resolution of the DØ detector. The generated resonance is forced to decay into  $t\bar{t}$ .

For Run IIb, the standard model  $t\bar{t}$  is generated with ALPGEN [21] for generating the partons and PYTHIA 6.409 for fragmentation. For  $t\bar{t}$  events in Run IIa PYTHIA 6.323 was used for both. Diboson backgrounds ( $WW$ ,  $WZ$  and  $ZZ$ ) were generated with PYTHIA 6.323. For generating kinematic distributions for  $t\bar{t}$  pairs a top quark mass of 170 GeV was used for Run IIb and 175 GeV for Run IIa, for both resonant and  $t\bar{t}$  production processes. The single top quark production was generated using the COMPHEP generator [22]. For single top and diboson production the Run IIa MC were used.  $W$ +jets and  $Z$ +jets events were generated using ALPGEN [21] to model the hard interaction and PYTHIA 6.409 and PYTHIA 6.323 respectively for parton showering, hadronization and hadron decays. To avoid double counting between the hard matrix element and the parton shower the MLM jet-matching algorithm was used [23]. For all samples the PDF set CTEQ6L1 was applied. The generated events have been processed through the full GEANT3-based [24] DØ detector simulation and the same reconstruction program used for data.

The MC-generated SM backgrounds are used both to obtain the total acceptance and the shape of the reconstructed  $t\bar{t}$  invariant mass distribution. Trigger and reconstruction inefficiencies are accounted for by weighting the simulated events. Jet  $b$ -tagging probabilities are measured in data and parametrized as function of  $p_T$  and  $\eta$ . They are used to weight each simulated event according to its event  $b$ -tagging probability. Finally, the expected yields are normalized to the SM theoretical prediction. For the  $t\bar{t}$  production  $\sigma_{t\bar{t}} = 7.31$  pb for  $m_t = 172.5$  GeV [25] is used for both Run IIa and Run IIb. Single top and diboson samples are normalized to their NLO cross-sections [26, 27]. For  $Z$ +jets the LO generator cross-sections are corrected to NLO using  $K$ -factors of 1.35 (1.66) for  $Z$ +light partons ( $Z + c\bar{c}$  and  $Z + b\bar{b}$ ).

The  $W$ +jets background is estimated from a combination of data and MC information. The expected number of  $W$ +jets events in the  $b$ -tagged sample is computed as the product of the estimated number of  $W$ +jets before  $b$ -tagging and the expected event  $b$ -tagging probability. The former is obtained from the observed number of events with real leptons in data, computed using the Matrix Method [15], and then subtracting the expected contributions from other SM production processes. The  $b$ -tagging probability is obtained by combining the  $W$ +jets flavor fractions estimated from MC with the event  $b$ -tagging probability, estimated from  $b$ -tag rate functions. The shape of the reconstructed invariant mass distribution is obtained from the MC simulation.

The multijet background is determined from data. The total number of expected events is estimated by applying the Matrix Method on the  $b$ -tagged sample. The shape is derived from events with leptons failing the isolation requirements.

#### V. RECONSTRUCTION OF THE $t\bar{t}$ INVARIANT MASS DISTRIBUTION

The  $t\bar{t}$  invariant mass is reconstructed from the four-momenta of up to four leading jets, the lepton momentum and the neutrino momentum. The latter is obtained from the transverse missing energy,  $\cancel{E}_T$ , and by solving  $M_W^2 = (p^l + p^\nu)^2$  for the component of the neutrino  $p$  momentum along the beam direction, using  $\cancel{E}_T$  for the neutrino transverse momentum. If there are two solutions, the one with the smaller  $|p_z^\nu|$  is taken; if no solution exists,  $p_z^\nu$  is set to 0. This method was shown to give better sensitivity for high mass resonances than a previously applied constrained kinematic fit technique [7], while only slightly reducing the sensitivity for lower resonance masses. Moreover, this direct reconstruction allows the inclusion of data with fewer than four jets in the case that some jets are merged,

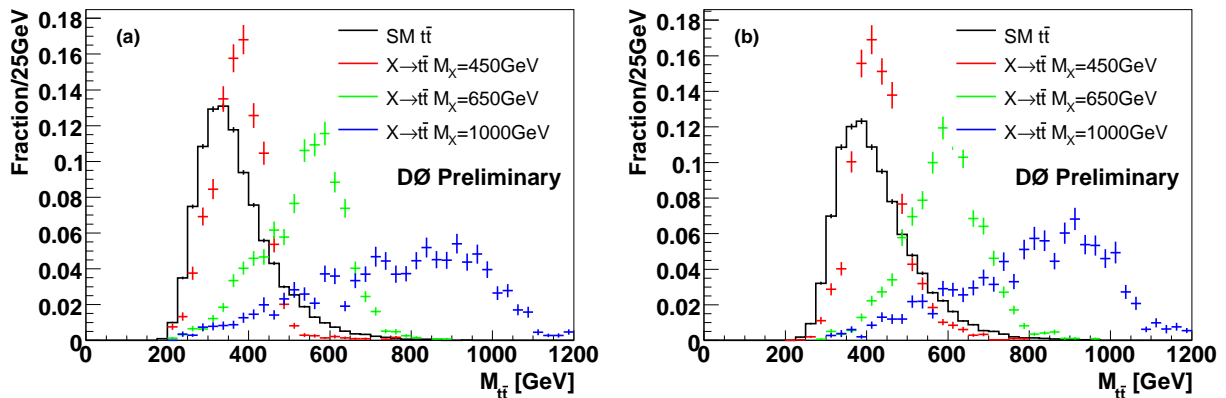


FIG. 1: Shape comparison of expected  $t\bar{t}$  invariant mass distribution for Run IIB data set for standard model top pair production (histogram) compared to resonant production from narrow-width resonances of mass  $M_X = 450$ ,  $650$  GeV, and  $M_X = 1$  TeV (left to right), for 3 jet events (a) and  $\geq 4$  jet events (b). The expected shape distributions for Run IIA can be seen in Fig. 9 in [9].

further increasing the sensitivity. The expected  $t\bar{t}$  invariant mass distributions for three different resonance masses are compared to the SM expectation in Fig. 1.

## VI. SYSTEMATIC UNCERTAINTIES

The systematic uncertainties can be classified as those affecting only normalization and those affecting the shape of any of the signal or background invariant mass distribution. The systematic uncertainties affecting only the normalization include the theoretical uncertainty on the SM prediction for  $\sigma_{t\bar{t}}$ , the uncertainty on the integrated luminosity (6.1%) [28] and the uncertainty of lepton identification efficiencies.

The systematic uncertainties affecting the shape of the  $t\bar{t}$  invariant distribution as well as the normalization have been determined for both signal and background samples. These include uncertainties on the jet energy calibration, jet reconstruction efficiency and  $b$ -tagging parametrizations for  $b$ ,  $c$  and light quark jets. The central  $t\bar{t}$  cross-section of  $7.31$  pb, appropriate for  $m_t = 172.5$  GeV, is taken with an error of  $^{+0.88}_{-0.86}$  to obtain the systematic uncertainty on the  $t\bar{t}$  background normalization. The systematic uncertainty on the  $t\bar{t}$  invariant mass distribution shape is obtained by varying the top quark mass for Run IIA between  $165$  and  $185$  GeV, and for Run IIB between  $165$  and  $175$  GeV, and taking half this variation to obtain the  $1\sigma$  errors for each of the two samples to take into account uncertainties on the top quark mass. Note that we separate the normalization error due to the cross-section uncertainty and the shape error due to top mass uncertainty.

The fraction of heavy flavor in the  $W$ +jets background has been measured in control samples and a corresponding uncertainty on the  $W$ +jets flavor composition is determined. Also the uncertainties of tuning the parameterization of the  $b$ -fragmentation function, and the uncertainties of the efficiencies used in the Matrix Method were propagated to the limit setting.

Table I gives a summary of the relative systematic uncertainties on the total SM background normalization for the combined  $\ell$ +jets channels in Run IIB. Run IIA values can be found in [9]. The effect of the different systematic uncertainties, for both electron and muon channels, on the shape of the  $t\bar{t}$  invariant mass distribution can not be inferred from this table.

## VII. RESULT

After all selection cuts  $731$  events remain in the  $e$ +jets channel and  $565$  events in the  $\mu$ +jets channel. The sums of all standard model and multijet instrumental backgrounds are  $692 \pm 26$  and  $524 \pm 23$  events, respectively. The event yields for the data and background sources are indicated in Table II. Invariant mass distributions are computed for events with exactly one  $b$ -tag and for events with more than one  $b$ -tag. Additionally, the distributions are separated into 3 jet and 4 or more jet samples, as well as Run IIA and Run IIB data ranges. The measured invariant mass distributions and corresponding background estimations are shown in Fig. 2 for the 3 and  $\geq 4$  jet samples for both Run IIA and Run IIB.

Source	SM processes (backgrounds)		Resonance $M_X = 650$ GeV	
	3 jets	$\geq 4$ jets	3 jets	$\geq 4$ jets
Jet energy calibration	$\pm 0.6\%$	$\pm 3.9\%$	$\pm 3.0\%$	$\pm 4.6\%$
Jet energy resolution	$\pm 0.1\%$	$\pm 0.0\%$	$\pm 0.8\%$	$\pm 0.1\%$
Jet identification	$\pm 0.2\%$	$\pm 1.0\%$	$\pm 0.3\%$	$\pm 1.8\%$
$\sigma_{t\bar{t}}(m_t = 170$ GeV)	$\pm 4.8\%$	$\pm 7.7\%$	–	–
Top quark mass	$\pm 0.2\%$	$\pm 2.1\%$	–	–
$b$ -tagging	$\pm 4.6\%$	$\pm 7.0\%$	$\pm 4.6\%$	$\pm 4.1\%$
$b$ fragmentation	$\pm 1.3\%$	$\pm 0.9\%$	$\pm 0.4\%$	$\pm 0.3\%$
$W$ +jets (heavy flavor)	$\pm 3.0\%$	$\pm 1.1\%$	–	–
Multijet lepton fake rate	$\pm 0.2\%$	$\pm 0.2\%$	–	–
Selection efficiencies	$\pm 3.2\%$	$\pm 5.1\%$	$\pm 3.6\%$	$\pm 3.6\%$
Luminosity	$\pm 2.5\%$	$\pm 3.9\%$	$\pm 6.0\%$	$\pm 6.1\%$

TABLE I: The relative systematic errors on the overall normalization of the standard model background, and for a resonance mass of  $M_X = 650$  GeV, with at least one  $b$ -tagged jet for Run IIb and Run IIa combined, and the normalization errors were symmetrized for simplicity of presentation. The actual asymmetric errors and the effect of shape variation systematic errors were used in the limit setting.

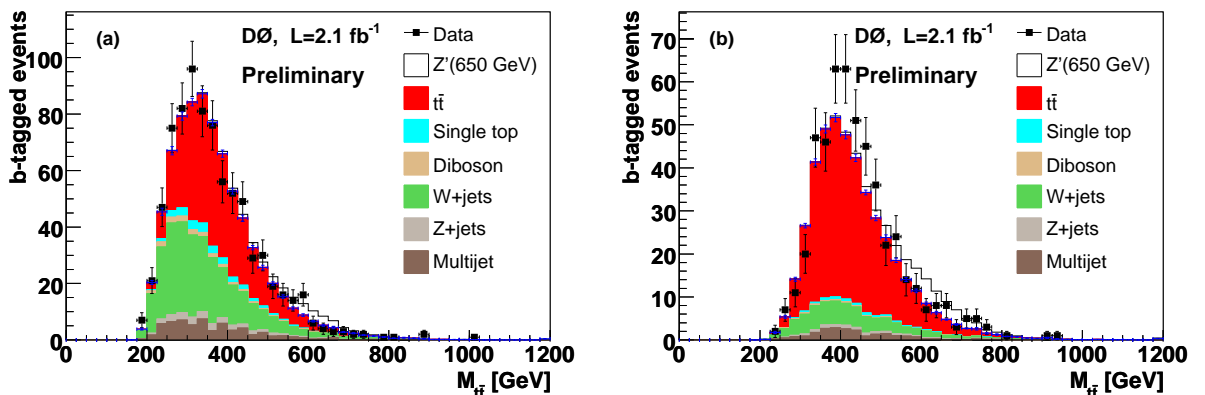


FIG. 2: Expected and observed  $t\bar{t}$  invariant mass distribution for the combined  $\ell + 3$ jets (a), and  $\ell + 4$  or more jets channels (b), with at least one identified  $b$ -jet. The error bars drawn on top of the SM background indicate the statistical uncertainty. Superimposed as white area is the theory signal for a top-color-assisted technicolor  $Z'$  boson with  $M_{Z'} = 650$  GeV. The number of data, signal and expected background events from each source are indicated in Table II.

Finding no significant deviation from the standard model expectation, a Bayesian approach is applied to calculate 95% C.L. upper limits on  $\sigma_X \cdot B(X \rightarrow t\bar{t})$  for hypothesized values of  $M_X$  between 350 and 1000 GeV. A Poisson distribution is assumed for the number of observed events in each bin, and flat prior probabilities are taken for the signal cross-section times branching fraction. The prior for the combined signal acceptance and background yields is a multivariate Gaussian with uncertainties and correlations described by a covariance matrix [29].

The expected and observed 95% C.L. upper limits on  $\sigma_X \cdot B(X \rightarrow t\bar{t})$  as a function of  $M_X$ , after combining the

	3 jet	$\geq 4$ jets
$t\bar{t}$ jets	364	344
Single top	27	7
Diboson	18	4
$W$ +jets	272	60
$Z$ +jets	27	9
Multijet	62	22
Total background	770	446
Data	791	505

TABLE II: Event yields from data and for the SM expectation.

$M_X$ [GeV]	exp. limit [pb]	obs. limit [pb]
350	1.47	1.88
400	1.46	1.52
450	1.30	1.43
500	1.12	1.03
550	0.85	0.73
600	0.61	0.67
650	0.48	0.66
750	0.32	0.43
850	0.25	0.29
1000	0.20	0.21

TABLE III: Expected and observed limits for  $\sigma_X \cdot B(X \rightarrow t\bar{t})$  at the 95% confidence level when combining all channels and taking all systematic uncertainties into account.

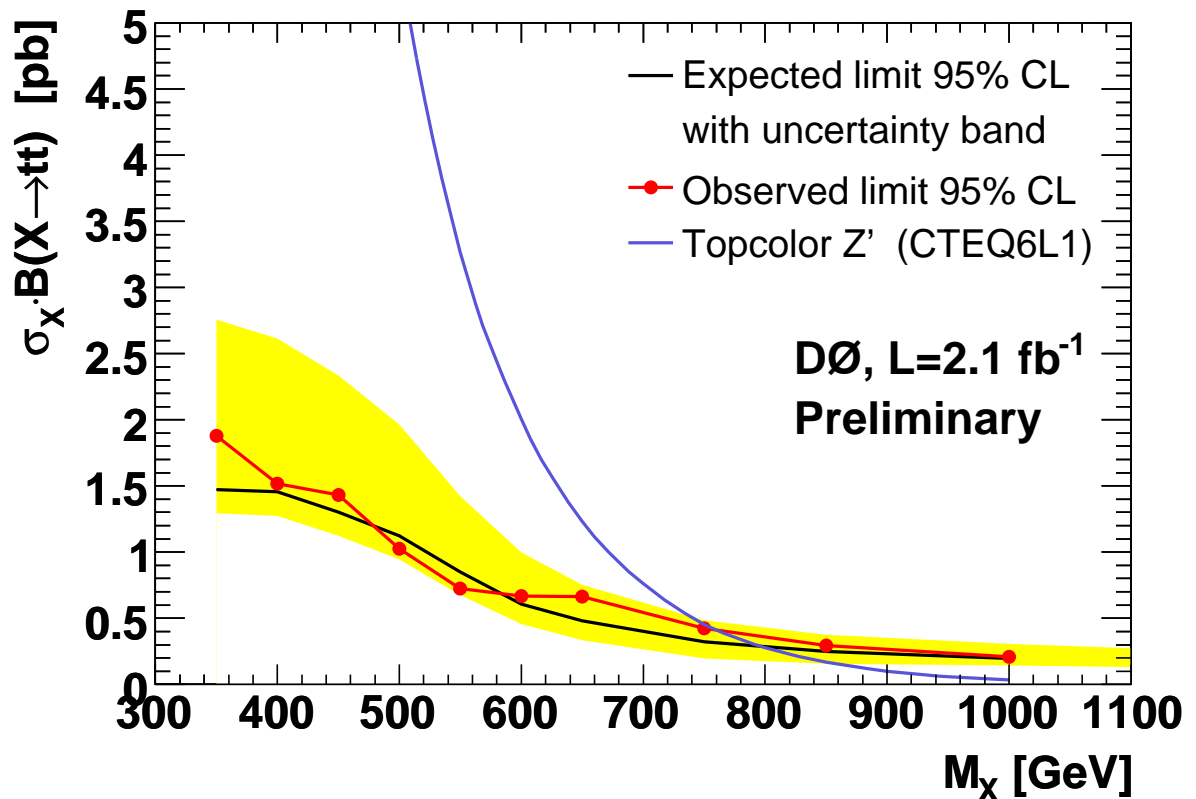


FIG. 3: Expected and observed 95% C.L. upper limits on  $\sigma_X \cdot B(X \rightarrow t\bar{t})$  compared with the predicted top-color-assisted technicolor cross-section for a  $Z'$  boson with a width of  $\Gamma_{Z'} = 0.012M_{Z'}$  as a function of the resonance mass  $M_X$ . The shaded band gives the  $\pm 1\sigma$  uncertainty in the SM expected limit.

1 and 2  $b$ -tag samples and the 3 and  $\geq 4$  jet samples, are summarized in Table III and displayed in Fig. 3. This figure also includes the predicted  $\sigma_X \cdot B(X \rightarrow t\bar{t})$  for a leptophobic  $Z'$  boson with  $\Gamma_{Z'} = 0.012M_{Z'}$  computed using CTEQ6L1 parton distribution function. The expected limit for the  $Z'$  boson is 795 GeV. The comparison of the observed cross-section limits with the  $Z'$  boson prediction excludes  $M_{Z'} < 760$  GeV at 95% C.L.

## VIII. CONCLUSION

A search for a narrow-width heavy resonance decaying to  $t\bar{t}$  in the  $\ell$ +jets final states has been performed using data corresponding to an integrated luminosity of about  $2.1 \text{ fb}^{-1}$ , collected with the D0 detector at the Tevatron collider.

By analyzing the reconstructed  $t\bar{t}$  invariant mass distribution and using a Bayesian method, model independent upper limits on  $\sigma_X \cdot B(X \rightarrow t\bar{t})$  have been obtained for different hypothesized masses of a narrow-width heavy resonance decaying into  $t\bar{t}$ . Within a top-color-assisted technicolor model, the existence of a leptophobic  $Z'$  boson with  $M_{Z'} < 760$  GeV and widths around  $\Gamma_{Z'} = 0.012M_{Z'}$  can be excluded at 95% C.L.

- 
- [1] A. Leike, “The phenomenology of extra neutral gauge bosons,” Phys. Rept. 317 (1999) 143.
  - [2] B. Lillie, L. Randall, and L.-T. Wang, “The bulk RS KK-gluon at the LHC,” JHEP 09 (2007) 074.
  - [3] T. G. Rizzo, “Testing the nature of kaluza-klein excitations at future lepton colliders,” Phys. Rev. D 61 (2000) 055005.
  - [4] L. M. Sehgal and M. Wanninger, “Forward - backward asymmetry in two jet events: Signature of axigluons in proton - anti-proton collisions,” Phys. Lett. B 200 (1988) 211.
  - [5] C. T. Hill and S. Parke, “Top production: sensitivity to new physics,” Phys. Rev. D 49 (1994) 4454.
  - [6] CDF Collaboration, T. Affolder et al., “Search for new particles decaying to  $t\bar{t}$  in  $p\bar{p}$  Collisions at  $\sqrt{s} = 1.8$  TeV,” Phys. Rev. Lett. 85 (2000) 2062.
  - [7] DØ Collaboration, V. Abazov et al., “Search for Narrow  $t\bar{t}$  Resonances in  $p\bar{p}$  Collisions at  $\sqrt{s} = 1.8$  TeV,” Phys. Rev. Lett. 92 (2004) 221801.
  - [8] R. M. Harris, C. T. Hill, and S. Parke, “Cross section for Topcolor  $Z'$  decaying to  $t\bar{t}$ ,” hep-ph/9911288, 1999.
  - [9] DØ Collaboration, V. Abazov et al., “Search for  $t\bar{t}$  Resonances in the Lepton+Jets Final State in  $p\bar{p}$  Collisions at  $\sqrt{s} = 1.96$  TeV,” DØ Note 5443-CONF, 2007.
  - [10] CDF Collaboration, T. Aaltonen et al., “Search for resonant  $t\bar{t}$  production in  $p\bar{p}$  collisions at  $\sqrt{s} = 1.96$  TeV,” arXiv:0709.0705 [hep-ex], 2007.
  - [11] CDF Collaboration, T. Aaltonen, “Limits on the production of narrow  $t\bar{t}$  resonances in  $p\bar{p}$  collisions at  $\sqrt{s} = 1.96$  TeV,” arXiv:0710.5335 [hep-ex], 2007.
  - [12] D0 Collaboration, V. M. Abazov et al., “The upgraded D0 detector,” Nucl. Instrum. Meth. Phys. Res. A 565 (2006) 463.
  - [13] D0 Collaboration, S. Abachi et al., “The D0 detector,” Nucl. Instrum. Meth. Phys. Res. A 338 (1994) 185.
  - [14] V. M. Abazov et al., “The muon system of the Run II D0 detector,” Nucl. Instrum. Meth. Phys. Res. A 552 (2005) 372.
  - [15] D0 Collaboration, V. M. Abazov et al., “Measurement of the  $t\bar{t}$  production cross section in  $p\bar{p}$  collisions at  $\sqrt{s} = 1.96$  TeV using kinematic characteristics of lepton + jets events,” Phys. Lett. B 626 (2005) 45.
  - [16] D0 Collaboration, V. M. Abazov et al., “Measurement of the  $t\bar{t}$  production cross section in  $p\bar{p}$  collisions at  $\sqrt{s} = 1.96$  TeV using lepton + jets events with lifetime b-tagging,” Phys. Lett. B 626 (2005) 35.
  - [17] G. Blazey et al., in “QCD and weak boson physics in Run II”, U. Baur, R. K. Ellis, and D. Zeppenfeld, Eds., FERMILAB-PUB-00-297, 2000.
  - [18] A. Scharzmann and C. Tully, “Improving calorimeter jet resolution using tracks,” CMS Jet Met Meeting @ LPC, June 29, 2005.
  - [19] T. Scanlon, “ $b$ -tagging and the search for neutral supersymmetric Higgs bosons at D0,” FERMILAB-THESIS-2006-43.
  - [20] T. Sjostrand, L. Lonnblad, and S. Mrenna, “PYTHIA 6.2: Physics and manual,” hep-ph/0108264, 2001.
  - [21] M. L. Mangano, M. Moretti, F. Piccinini, R. Pittau, and A. D. Polosa, “ALPGEN, a generator for hard multiparton processes in hadronic collisions,” JHEP 07 (2003) 001.
  - [22] E. E. Boos, V. E. Bunichev, L. V. Dudko, V. I. Savrin, and A. V. Sherstnev, “Method for simulating electroweak top-quark production events in the nlo approximation: Singletop event generator,” Phys. Atom. Nucl. 69 (2006) 1317.
  - [23] S. Höche et al., “Matching parton showers and matrix elements,” hep-ph/0602031, 2006.
  - [24] R. Brun and F. Carminati, CERN Program Library Long Writeup W5013, 1993.
  - [25] N. Kidonakis and R. Vogt, Eur. Phys. J. C 33 (2004) 466.
  - [26] Z. Sullivan, “Understanding single-top-quark production and jets at hadron colliders,” Phys. Rev. D 70 (2004) 114012.
  - [27] J. M. Campbell and R. K. Ellis, “An update on vector boson pair production at hadron colliders,” Phys. Rev. D 60 (1999) 113006.
  - [28] T. Andeed et al., “Determination of the effective inelastic  $p\bar{p}$  cross-section for the D0 Run II luminosity measurement,” FERMILAB-TM-2365, 2007.
  - [29] I. Bertram et al., “A recipe for the construction of confidence limits,” FERMILAB-TM-2104.